

# Obscuration in the Host Galaxies of Soft X-ray Selected Seyferts

Robert Simcoe<sup>1</sup>, K. K. McLeod, Jonathan Schachter, Martin Elvis

*Smithsonian Astrophysical Observatory, 60 Garden St., Cambridge, MA 02138*

*rasimcoe@phoenix.princeton.edu*

*kmcleod, jschachter, & melvis@cfa.harvard.edu*

## ABSTRACT

We define a new sample of 96 low-redshift ( $z < 0.1$ ), soft X-ray selected Seyferts from the catalog of the *Einstein* Slew Survey (Elvis et al. 1992, Plummer et al. 1994). We probe the geometry and column depth of obscuring material in the host-galaxy disks using galaxian axial ratios determined mainly from the Digitized Sky Survey. The distribution of host-galaxy axial ratios clearly shows a bias against edge-on spirals, confirming the existence of a geometrically thick layer of obscuring material in the host-galaxy planes. Soft X-ray selection recovers some of the edge-on objects missed in UV and visible surveys but still results in 30% incompleteness for Type 1's. We speculate that thick rings of obscuring material like the ones we infer for these Seyferts might be commonly present in early type spirals, sitting at the Inner Lindblad Resonances of the nonaxisymmetric potentials of the host galaxies.

*Subject headings:* galaxies: Seyfert—galaxies: nuclei—galaxies: structure—Xrays: galaxies

---

<sup>1</sup>Princeton University Observatory, Peyton Hall, Princeton, NJ 08544

## 1. Introduction

In studies of active galactic nuclei (AGN), much attention has been paid to “unified” schemes (e.g. Antonucci & Miller 1985; Antonucci 1993) that explain the observed differences among the classes of Seyferts based on our viewing angle to the nucleus. In these models, an optically thick torus with a radius of about 1 pc surrounds the broad line region (BLR). When our line of sight intercepts this torus, the central continuum source and the BLR are hidden from our view and we see only the Type 2 spectrum from the narrow line region (NLR).

Far fewer investigations have focused on obscuration on a larger scale. Keel (1980) found that optically-selected (mostly Type 1) Seyferts tend to avoid host galaxies with axial ratio  $b/a < 0.5$ , i.e. they are rarely found in edge-on galaxies. By contrast, hard X-ray (2-10 keV) selected Seyferts show no such bias (Lawrence & Elvis 1982). Lawrence & Elvis concluded that optically-selected samples must suffer biases due to obscuration in a flattened configuration parallel to the disk of the host galaxy. This and subsequent studies indicated that the obscuring material is likely inside or at the outer edge of the BLR (e.g. De Zotti & Gaskell 1985), though a more recent look suggested that the obscuring material might extend into the NLR (Kirhakos & Steiner 1990a).

To investigate this question further and to avoid the problems intrinsic to studying heterogeneous samples, McLeod & Rieke (1995) compiled statistics on several sets of AGN selected in different wavelength regimes. They found an excess of face-on spirals hosting both Type 1 and Type 2 AGN for a spectroscopically-selected sample. Therefore, a significant amount of dust in the galaxy plane must cover at least part of the NLR, i.e.,  $A_V \gtrsim$  several magnitudes out to  $r \gtrsim 100$  pc. They also found an excess of face-on spirals hosting soft X-ray selected AGN, and used it to estimate the column density along the

line of sight to the X-ray continuum source, inferring  $N_H \sim 10^{23} \text{ cm}^{-2}$  at scales  $r > 1$  pc. In both regimes, the aspect ratio (i.e. height-to-thickness) of the obscuring material is  $\approx 1$ .

A recent investigation by Maiolino & Rieke (1995) provides preliminary evidence that this additional component of obscuration might explain the axial ratio distributions and the spectral characteristics of intermediate Seyferts. In their model, a line of sight that intercepts the plane of the galaxy but not the inner torus would make a Seyfert 1 appear as a 1.8 or 1.9 (see their Figure 6). Maiolino & Rieke (1995) also present a theoretical model for the origin of geometrically thick, 100 pc-scale obscuring material in the context of tidal disruption of giant molecular clouds approaching the central compact object.

We stress that the galaxy inclination statistics are telling us about obscuring material that is distinct from, and not necessarily aligned with, the canonical torus of unification models. Radio maps and Hubble Space Telescope images indicate that the pc-scale torus of the unified model is not preferentially aligned with the larger scale galaxy disk (Schmitt et al. 1996; Wilson & Tsvetanov 1994; Ulvestad & Wilson 1984). Seyfert 2’s are often found in face-on spiral disks— and in the unified model, this means that the torus is in fact perpendicular to the host-galaxy disk.

The strongest limit placed by McLeod & Rieke (1995) on the column density in the galaxy’s disk was based on a sample of AGN serendipitously discovered by the *Einstein* IPC and reported by Malkan, Margon, & Chanan (1984). However, the Malkan et al. selection process might have eliminated *a priori* edge-on galaxies for which the X-rays got through but for which emission lines were absorbed, thus precluding their identification as AGN. In this paper, we use a new, complete, well-defined, soft X-ray sample of AGN from the *Einstein* Slew Survey (Elvis et al. 1992; Plummer et al. 1994). We measure axial ratios

from Digitized Sky Survey (DSS<sup>2</sup>) images and from new CCD images. This soft X-ray sample allows us to probe column densities in between those previously examined in UV-excess and hard X-ray samples.

## 2. Sample Selection

Our sample was chosen from the catalog of the *Einstein* Slew Survey in the soft X-ray band of 0.2-3.5 keV (Elvis et al. 1992, Plummer et al. 1994). This survey has a flux limit of approximately  $3 \times 10^{-12} \text{ erg cm}^{-2} \text{ s}^{-1}$  (Elvis et al. 1992) and is well-suited for defining a sample because of its extensive sky coverage. It maps about 50% of the sky, and contains 809 sources, 147 of which are classified as AGN. The objects were identified as AGN by correlation with pre-existing catalogs, or by examination of new spectra (Perlman et al. 1996; Huchra, Schachter, & Remillard private communication).

The most important requirement for our sample is that the objects be nearby enough to resolve the host galaxy of the AGN in DSS images, because undersampling can lead to errors in axial ratio measurements. We restricted our sample to Slew Survey AGN with  $z < 0.1$ , leaving us with 96 objects. The mean and median redshift for

this final sample is  $z = 0.042$ , at which distance a galaxy diameter of 25 kpc corresponds to an angle of  $34''$  ( $H_0 = 80 \text{ km/s/Mpc}$ ). This is approximately the size of  $D_{25}$ , the diameter at the  $B=25 \text{ mag/square arcsec}$  isophote, for a typical spiral galaxy.

Although the Slew Survey objects have been mostly identified, there still remain 129 objects without known optical counterparts. We examined DSS images of all of these fields to make sure that there are not significant numbers of  $z < 0.1$  AGN among the unidentified objects. We checked within the 95% confidence limit of the *Einstein* position ( $2'$  radius; Elvis et al. 1992) for galaxies with apparent sizes  $\geq 15''$ , or approximately  $D_{25}$  for a  $z = 0.1$  galaxy. There were only three galaxies satisfying these criteria, and only one of these three is edge-on. We conclude that our sample is at least 97% complete for  $z < 0.1$ , and that there is an insignificant number of potentially active edge-on galaxies with  $z < 0.1$  among the unidentified fields of the Slew Survey.

A more subtle concern in our sample selection was the identification of 35 Slew Survey objects that were classified as “normal” (i.e. non-AGN) galaxies. We are testing for obscuring material in the galaxy’s disk that can hide emission from the nuclear region. It is possible that X-rays from an AGN could penetrate this obscuring material, whereas visible light would be attenuated enough to hide the emission lines we use to identify an AGN. If this were the case, we would expect to observe many Slew Survey “normal” galaxies to be hidden AGN seen at high inclination. To test this possibility, we determined axial ratios for 20 of the 26 non-AGN spiral galaxies identified in the Slew Survey (the other 6 were too small, nebulous, or disturbed for a reliable measurement). The highly inclined members of this population are not likely to be hidden AGN—the 4 objects with  $b/a < 0.45$  are: the well-known starburst galaxies M82 and NGC253, the very nearby galaxy NGC2903, and the Andromeda

---

<sup>2</sup>Northern hemisphere based on photographic data of the National Geographic Society – Palomar Observatory Sky Survey (NGS-POSS) obtained using the Oschin Telescope on Palomar Mountain. The NGS-POSS was funded by a grant from the National Geographic Society to the California Institute of Technology. Southern hemisphere based on photographic data obtained using The UK Schmidt Telescope. The UK Schmidt Telescope was operated by the Royal Observatory Edinburgh, with funding from the UK Science and Engineering Research Council, until 1988 June, and thereafter by the Anglo-Australian Observatory. Original plate material is copyright (c) the Royal Observatory Edinburgh and the Anglo-Australian Observatory. All plates were processed into the present compressed digital form with permission from the National Geographic Society, Royal Observatory, and The AAO. The Digitized Sky Survey was produced at the Space Telescope Science Institute under US Government grant NAG W-2166.

Galaxy (M31). We conclude that there are not significant numbers of AGN with edge-on galaxies hidden in this subsample.

The final AGN sample is listed in Table 1. Catalog designations, axial ratios, and redshifts were extracted from NED<sup>3</sup> when available, and supplemented with data from new spectra obtained as part of the Slew Survey follow-up. We mark in Table 1 the 19 objects with  $z < 0.1$  that were not known as AGN before the Slew Survey. Of the 96 AGN in our sample, only seven are known or probable Type 2's (Table 1). Such a small fraction of Seyfert 2's in a soft X-ray sample is not surprising given the known high X-ray absorption columns through the pc-scale torus ( $N_H > 10^{23}$ ; Awaki et al. 1991).

### 3. Axial Ratios

Visible images of all galaxies in the sample were extracted from the DSS using the software package *GetImage*.<sup>4</sup> The digitized images had a resolution of  $1''.7$  per pixel, with typical FWHM in the range of  $3''.6$ . Previous studies of galaxy inclination statistics (Binney & deVaucouleurs 1981) have measured isophotes out to  $D_{25}$  so we tested our images to ensure we could measure isophotes at least as far. Comparison of northern hemisphere DSS images with CCD test images from the  $48''$  telescope at the Fred Lawrence Whipple Observatory (FLWO) on Mt. Hopkins, AZ, showed that the northern DSS outer isophotes reach regions of surface brightness corresponding to  $B \approx 25.3$  mag arcsec<sup>-2</sup>. The southern hemisphere DSS plates go slightly deeper, so all of the DSS images are of an appropriate depth for this work. For four of the objects (denoted '\*\*\*' in Table 1), we computed axial

ratios based on H-band images from McLeod & Rieke (1994). These objects are fairly distant and have very bright nuclei, so the high-resolution deep images were used to obtain better accuracy.

The images were all processed using the *ellipse* task in IRAF to fit elliptical isophotes at increasing radii to each galaxy. The isophote fits were carried out to the level at which the average signal in an isophote was slightly larger than the rms deviation of the flux in the isophote, i.e. signal-to-noise approximately unity. The outermost ellipses were used to determine the axial ratio of the host galaxy. On average, the formal ellipticity error generated by the fitting algorithm was  $\pm 0.086$ , which is greater than the difference in  $b/a$  between consecutive isophotes at outer radii. The axial ratios are given in Table 1. For about 25% of the sample, we were unable to measure a reliable axial ratio. In five cases a foreground object contaminated the galaxy (denoted "f" in Table 1). In 16 cases the object was too small or stellar ("s"); all of these are substantially more distant than the median redshift for the sample. In five additional cases the object was morphologically peculiar or interacting ("m"). For six very nearby galaxies that were bigger than our images we simply adopted the NED value of  $b/a$ . A histogram of axial ratios of the remaining 74 galaxies is shown in Figure 1a. There is an obvious deficiency of galaxies with small axial ratios.

One test of the accuracy of our fits is to compare our ratios to those objects in the sample with previously measured axial ratios found in NED (usually from the Third Reference Catalogue of Bright Galaxies, deVaucouleurs et al. 1991, hereafter RC3) and listed in Table 1. The axial ratio agreement is excellent: the difference between our value and NED's value has a mean of 0.02 and standard deviation of 0.12, as expected from the ellipse fitting uncertainties. We conclude that our axial ratios are accurate to  $b/a \approx 0.1$ . Two of the three most discrepant points are easily reconciled: the multiple "nuclei" of interacting galaxy 1ES0655+542 bias the mea-

<sup>3</sup>The NASA/IPAC Extragalactic Database (NED) is operated by the Jet Propulsion Laboratory and the California Institute of Technology, under contract with the National Aeronautics and Space Administration

<sup>4</sup>*GetImage* was created by J.Doggett for the Association of Universities for Research in Astronomy at the Space Telescope Science Institute, copyright AURA 1993

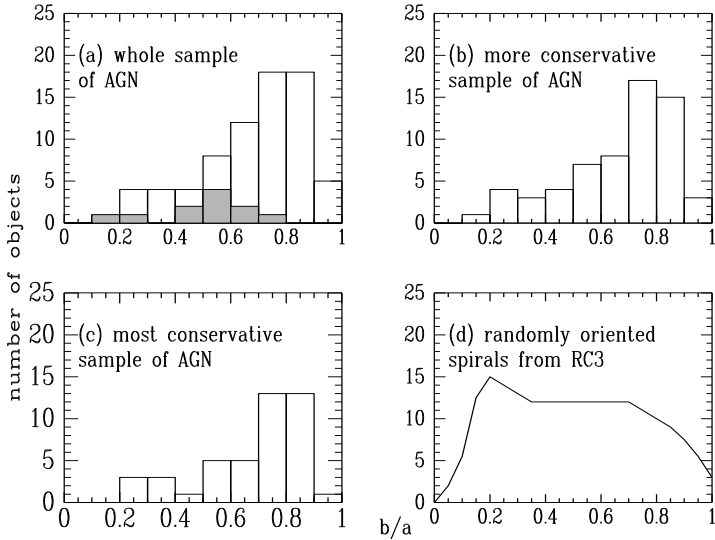


Fig. 1.— (a-c) Histograms of axial ratios for AGN from the *Einstein* Slew Survey (samples are explained in the text). The objects first identified as AGN by the Slew Survey are shown as filled bars. Even the most conservative AGN sample shows a strong bias against edge-on host galaxies. (d) Distribution for randomly oriented spiral galaxies from the RC3 catalog, adapted from Figure 3 of Fasano et al. 1993 and arbitrarily normalized for comparison.

surement so we discard this object from our final analysis; for 1ES0403–373 we noted that our resolution is poor, and hence we adopt the smaller NED value for the analysis. For 1ES0057+315, however, we see no obvious reason for a discrepancy. We believe our measurement is robust and use it in our analysis. The fraction of objects for which our axial ratios are larger than NED’s is too small to change the character of the  $b/a$  distribution.

The  $1''.7$  pixels of the DSS generally do not fully sample the seeing profiles of the original plates. To understand the effects of the POSS’s resolution limits for the more distant AGN in our sample, we obtained  $1''.5$  resolution CCD images at the FLWO 48” telescope for 10 of the more distant AGN (denoted ‘\*’ in Table 1). The average difference in  $b/a$  derived from POSS images

and CCD images was within the expected error margin of the ellipse fitting procedure. However, there is still the possibility that both sets of data undersample the galaxy images. We do see edge-on galaxies of similar size to the Seyfert hosts in the DSS images, but a bright Seyfert nucleus could artificially inflate the axial ratio for more distant objects. Figure 2 is a plot of the axial ratios of the galaxies in our sample versus their redshifts. The excess of round galaxies is seen for the whole range of  $z$  and is not solely a distance-dependent selection effect. However, the bias is possibly not as strong for  $z \geq 0.05$ , and many of the objects in that range have already been discarded by us because they were too compact for a reliable measurement. Therefore, we will define below a “most conservative sample” containing only the 44 objects with  $z < 0.05$ .

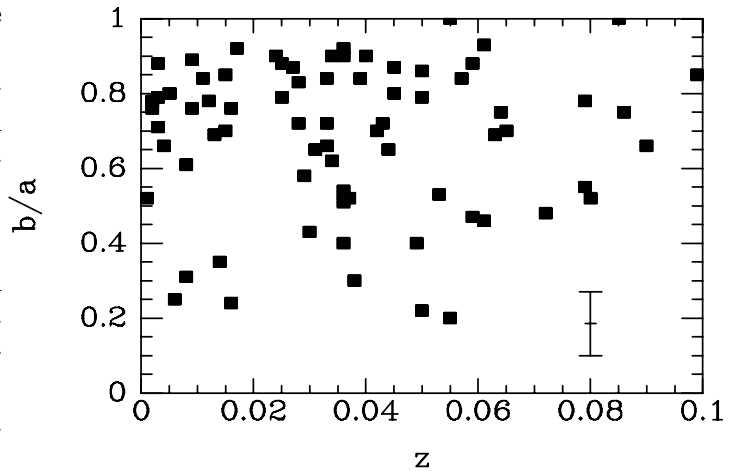


Fig. 2.— Distribution of axial ratios v. redshift for the whole sample. Typical  $\pm 1\sigma$  error bar is shown in lower right. Although the bias against hosts with axial ratios  $b/a \lesssim 0.6$  appears over the entire range of  $z$ , we exclude objects with  $z \geq 0.05$  from our most conservative sample.

#### 4. Results

Axial ratios for the “whole sample” of 74 AGN for which we have measurements are shown in Figure 1a. For comparison, we plot in Figure 1d

the distribution derived by Fasano et al. (1993) based on their analysis of  $> 1000$  randomly oriented spiral galaxies drawn from the RC3 catalog. The distribution shows a lack of galaxies with  $b/a < 0.15$ , due to the finite thickness of spiral disks. It also shows a dearth of galaxies with  $b/a > 0.8$ , interpreted as an effect of intrinsically triaxial disks. It is immediately obvious that the bias against edge-on hosts is strongly present in the soft X-ray sample; the distribution drops off considerably for  $b/a \lesssim 0.5 - 0.6$ , similar to what was seen for UV and spectroscopic (visible) samples. We find from a KS test that the soft X-ray sample axial ratios (Table 1) are different from those for randomly oriented spirals—the KS probability that the two distributions are consistent is only  $2 \times 10^{-9}$ . There is also an apparent lack of round galaxies, i.e. galaxies with  $b/a > 0.9$ .

This result persists in progressively more conservative subsamples. In Figure 1b we plot the distribution for a “more conservative” sample after removing 12 objects (Table 1) whose axial ratios might not be meaningful for disk galaxy statistics because the AGN is not in a simple disk galaxy (flagged by “m”), suffers from foreground contamination (flagged by “f”), or is a strong radio source that could be associated with an elliptical host galaxy (flagged by “r”). The KS probability that the axial ratio distribution for the resulting subsample is consistent with that for randomly oriented disks is  $2 \times 10^{-7}$ . Finally we remove the 18 remaining objects with  $z \geq 0.05$  (Figure 1c). The axial ratio distribution for this “most conservative” sample of 44 objects still shows a deficit of highly inclined galaxies, with a KS probability of  $3 \times 10^{-6}$  of being consistent with that for randomly oriented disks.

This result confirms the previous tentative result of McLeod & Rieke (1995) that soft X-ray selection suffers a bias against edge-on host galaxies. We estimate that the soft X-ray sample misses  $\approx 60\%$  of the AGN in galaxies with  $b/a < 0.6$ , corresponding to a missing fraction of

$\approx 30\%$  over all inclinations. These statistics apply to only the Seyfert 1’s—recall from §2 that Seyfert 2’s are not usually detected at all in soft x-ray samples.

The axial ratio  $b/a < 0.6$  corresponds to a galaxy inclination of  $i \gtrsim 55$  degrees, which determines the opening half-angle of the obscuring material coplanar with the host galaxy’s disk and implies a distribution of material with a thickness approximately equal to its distance from the galaxian center. The missing fraction implies a large covering factor for the soft X-ray absorber,  $f_c \gtrsim 0.6$  for  $i \gtrsim 55$  degrees.

The soft X-ray regime used to select the AGN used in our study allows us to put a stringent lower limit on the column density of obscuring material. For solar abundances and a typical AGN intrinsic photon spectrum of  $N(E) \propto E^{-1.7}$  (e.g. Petre et al. 1984) a column  $N_{\text{H}} \approx 10^{22} \text{ cm}^{-2}$  is required to give optical depth  $\tau = 1$  over the *Einstein* bandpass (Harris 1984). A previous hard X-ray study in the 2-10 keV band (Lawrence & Elvis 1982), which did not detect a bias toward face-on spirals, can be used to set an upper limit on  $N_{\text{H}}$ . To give  $\tau = 1$  for a typical 2 – 10 keV X-ray detector requires a column density of  $\sim 2 \times 10^{23} \text{ cm}^{-2}$  (using the MPC response in *PIMMS*, Mukai 1993). Hence, the obscuring material has column density in the range  $10^{22} < N_{\text{H}} < 2 \times 10^{23} \text{ cm}^{-2}$ . If we assume a standard Milky Way ratio of  $N_{\text{H}}/A_{\text{V}} = 1.9 \times 10^{21}$  (Savage & Mathis 1979), we obtain a corresponding visual extinction  $A_{\text{V}} = 5 - 100$  magnitudes.

## 5. Discussion

The bias against finding edge-on host galaxies seen in this soft X-ray selected AGN sample is detected at high confidence. However, it appears to be weaker than the biases seen in UV and visible samples. We have quantified the differences among axial ratio distributions of Seyferts selected in various wavelength regimes using the KS statistic to test the null hypothesis that two

distributions are drawn from the same parent distribution. Hard X-ray selection is represented by the complete, though small, hard X-ray sample described in Piccinotti et al. (1982) with axial ratios compiled by Kotilainen et al. (1992). Soft X-ray selection is represented by the Slew Survey “most conservative” sample in this paper. UV selection is represented by the Cheng (1985) sample of mostly Markarian Seyfert 1’s, with the axial ratios taken from Zitelli et al. (1993) and supplemented by us using values from the literature and DSS images. Visible spectroscopic selection is represented by the Huchra & Burg (1992) CfA Seyfert sample with axial ratios from McLeod & Rieke (1995).

We compare these samples with each other and with the distribution that would be expected from a sample of randomly oriented spirals, and we summarize the results in Table 2 and Figure 3. These tests confirm that only the hard X-ray sample distribution can be consistent with a distribution of randomly oriented disk galaxies, and that all other samples are biased against edge-on galaxies with KS probability  $< 3 \times 10^{-6}$ . The KS test cannot rule out that the soft X-ray and UV samples might be drawn from the same parent population. However, there are two suggestions that the soft X-ray sample is less biased than the UV sample. First, whereas the soft X-ray distribution might be consistent with the hard X-ray distribution (KS probability  $P = 0.358$ ), the UV distribution is less likely to be ( $P = 0.043$ ). A definitive test awaits a larger hard X-ray sample. Second, the new AGN discovered by the Slew Survey (shaded area in Figure 1a) tend to have axial ratios in the low  $b/a$  half of the distribution, implying that soft X-ray selection has found a fraction of the AGN that are missing from UV (and visible) surveys. It is therefore likely that the column density of the absorbing material is close to the lower limit derived above,  $N_{\text{H}} \approx 10^{22} \text{ cm}^{-2}$ , or  $A_{\text{V}} \approx 5 \text{ mag}$ , at least for inclinations near 55 degrees.

The obscuring material must lie outside the

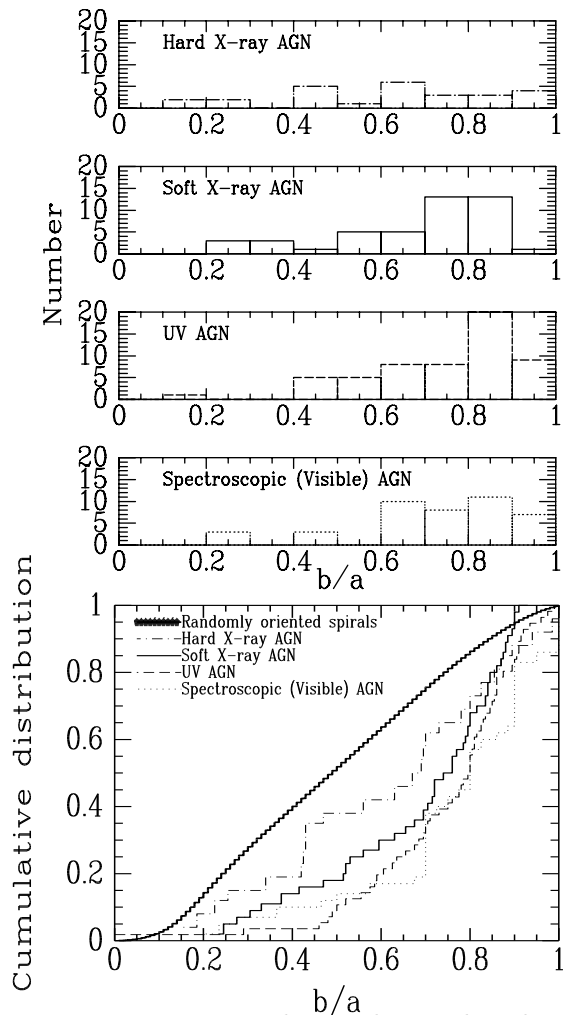


Fig. 3.— Histograms and cumulative distributions of axial ratios for samples described in the text.

soft X-ray emitting region of the AGN, but this is not a strong constraint. A substantial fraction (20-30%) of the soft X-ray emission of some Seyfert galaxies is found to be extended on a kpc scale (Morse et al. 1995). However, in these galaxies the observed direct soft X-ray continuum has been suppressed by nuclear absorption. The extended emission is no more than a few percent of the unabsorbed continuum flux, which is compact on sub-pc scales. McLeod & Rieke (1995) have already shown that material with at least several magnitudes of visual extinction and with the same orientation and thickness-to-height ra-

tio hides at least some of the NLR and so must lie at  $r \sim 100$  pc from the AGN’s center. It is likely that the X-ray and UV absorbing components are part of a continuous distribution of gas/dust clouds. In fact, if the column density to the X-ray source is close to our lower limit as suggested above, then most of the soft X-ray absorption can be accounted for by the same, 100 pc-scale material that hides the NLR.

Maiolino & Rieke (1995) have suggested that some Seyferts of Type 1.8-1.9 are actually Seyfert 1’s viewed through such a thick “outer torus” in the plane of the host galaxy. Obtaining high-quality visible spectra for the AGN discovered by the Slew Survey could help us to confirm this trend. To investigate the question further, though, we will need to find more AGN in edge-on galaxies. Hard X-ray selection and infrared selection remain good ways to locate the missing objects. Kirhakos & Steiner (1990a,b) combined hard X-ray and far-IR selection to locate new examples of AGN in edge-on hosts. However, if the amount of obscuring material is close to  $A_V \approx 5$  mag as we suggest, then the missing objects should be easily visible even in the near-IR where the extinction is lower by a factor of  $\sim 10$ . In addition, high-quality nuclear spectra in visible light can pick out partially-hidden AGN in edge-on galaxies in the nearest galaxies, where the sensitivity to nuclear emission is high because of their proximity (Maiolino & Rieke 1995; Ho 1996).

We note that a related result, namely a bias against edge-on host galaxies, has recently been found by Barth et al. (1996) for UV-bright LINERS. They find that the visibility drops for host inclinations  $> 65$  degrees, similar to that found for Seyferts. The good spatial resolution of the images (from WFPC2) shows dust lanes well inside the central kpc of the galaxies with several magnitudes of extinction (at  $2200\text{\AA}$ ). Similarly, an HST UV imaging survey of an unbiased sample of 110 nearby galaxies has turned up a tendency for UV “null emitters” to appear nearly

exclusively in galaxies with inclination  $> 60$  degrees, suggesting that the host-galaxy disks obscure what would otherwise be seen as UV “weak emitters” (Maoz et al. 1996).

As pointed out in McLeod & Rieke (1995) and Maiolino & Rieke (1995), direct evidence for a 100 pc-scale, geometrically thick distribution of molecular gas like the one we infer has been seen in several nearby AGN (e.g. Tacconi et al. 1994; Bergman et al. 1992; Israel et al. 1990; Rydbeck et al. 1993). The prevalence of this bias for samples of active and even mildly active nuclei suggests that a geometrically and optically thick distribution of gas and dust could be a common feature of the early-type disk galaxies in which they are generally found. The obscuring material would be more difficult to detect in galaxies where there is no bright, compact nucleus, especially given the required spatial resolution: 50 pc corresponds to  $\theta \approx 0''.5 \times (20 \text{ Mpc})/d$ . A high-resolution CO aperture synthesis study of the nearby, edge-on spiral NGC891 shows evidence for a relatively thick nuclear disk of molecular gas with  $r \sim 225$  pc in a normal galaxy (Scoville et al. 1993). The disk has thickness  $h \sim 160$  pc, within a factor of 1.5 as geometrically thick as we infer from the AGN axial ratios, and contains enough material to satisfy the optical depth requirement. There is so far no evidence that this molecular disk has a central hole to provide the required opening angle.

Maiolino & Rieke (1995) speculate that, for Seyferts, a distribution of obscuring material with a central hole might result from the tidal disruption of molecular clouds as they migrate inwards from the large-scale galaxy disk into the potential of the compact central object. Here we suggest a complementary model that naturally accounts for a central hole, namely that the gas is part of a nuclear ring of the type often associated with bars or oval distortions in early-type spirals. Nuclear star-forming rings have sizes on the order of several hundred pc and are probably associated with the Inner Lindblad Resonances



(ILRs) of the potential (Buta & Crocker 1993; Kenney 1996). Numerical simulations of barred galaxies show that the buildup of central mass results in the formation of a strong ILR. The gas transported inwards via radial orbits in the large-scale bar or oval distortion collects at the ILR, and even the cold gas there can have a geometrically thick distribution because of vertical resonances (Friedli & Benz 1993).

If this interpretation is correct, then we would expect the large scale galaxy disks to show evidence of the nonaxisymmetric potential. Indeed, the axial ratio distribution for the Slew Survey sample shows a strong deficit of galaxies with  $b/a > 0.9$  indicating a lack of round galaxies (Figure 1). Similar deficits were noted by Malkan, Margon, & Chanan (1984) for their soft X-ray sample, and by Maiolino & Rieke for their spectroscopic sample. The UV-excess sample in Figure 3 shows a similar but weaker bias. Because  $b/a$  cannot exceed unity, the effect of measurement uncertainties will tend to create a deficit in the last bin, but this effect should be relatively small given the accuracy of our measurements. However, the distributions for normal spiral galaxies also show a bias against perfectly round systems (Figure 1d; Binney & deVaucouleurs 1981; Fasano et al. 1993), and it is likely that disks of non-active galaxies are triaxial (Binney & deVaucouleurs 1981; Fasano et al. 1993; Rix & Zaritsky 1995). We cannot determine from our data whether the Seyfert hosts are less often perfectly round than those of non-active spirals, but the observed distribution suggests that this might be an interesting topic for future study.

## 6. Conclusions

We have defined a complete sample of *Einstein* Slew Survey AGN with  $z < 0.1$ . This sample comprises 96 mostly Type 1 AGN including 19 objects at  $z \approx 0.05$  not previously known to be active. The distribution of host-galaxy axial ratios clearly shows a bias toward face-on spirals,

confirming the existence of a geometrically thick layer of obscuring material in the host-galaxy planes. Combining this and other studies, we infer that this material is likely to be  $\sim 100$  pc from the nucleus with a thickness of  $\sim 100$  pc and column density of  $N_{\text{H}} = (1 - 20) \times 10^{22} \text{ cm}^{-2}$ , probably nearer the low end of this range for lines of sight near the edge of the  $\sim 55 - 60$  degree opening half-angle. The covering fraction of the soft X-ray absorbing material within this thick distribution is large, about 60%. Soft X-ray selection appears to recover some of the edge-on objects missed in UV and visible surveys but still results in an overall 30% incompleteness for Type 1's. We speculate that thick rings of obscuring material like the ones we infer for Seyferts might be commonly present in early type spirals, sitting at the Inner Lindblad Resonances of the nonaxisymmetric potentials of the host galaxies.

RAS thanks Smita Mathur for helpful discussions. KKM gratefully acknowledges financial support from NASA Grant NAGW-3134 (B. Wilkes, PI) and thanks Luis Ho for useful discussions. This work was also supported in part by NASA Grant NAG5-3066(ADP) and the SAO Summer Intern Program.

## REFERENCES

- Antonucci, R. R. J. 1993, *ARA&A*, 31, 473
- Antonucci, R. R. J. & Miller, J. S. 1985, *ApJ*, 297, 621
- Awaki, H., Koyama, K., Inoue, H., & Halpern, J. P. 1991, *PASJ*, 43, 195
- Barth, A. J., Ho, L. C., Filippenko, A. V., & Sargent, W. L. W. 1996, in press in *The Physics of LINERs in View of Recent Observations*, eds. Eracleous, M., Koratkar, A. P., Ho, L. C., & Leitherer, C. (San Francisco: ASP)
- Bergman, P., Aalto, S., Black, J. H., & Rydbeck, G. 1992, *A&A*, 265, 403

- Binney, J., & de Vaucouleurs, G. 1981, *MNRAS*194, 679
- Buta, R., & Crocker, D. A. 1993, *AJ*, 105, 1344
- Cheng, F., Danese, L., DeZotti, G., & Franceschini, A. 1985, *MNRAS*, 212, 857
- DeVaucouleurs, G., DeVaucouleurs, A., Corwin, H. G. Jr., Buta, R. J., Paturel, G., & Foqué, P. 1991, *Third Reference Catalog of Bright Galaxies* (New York: Springer)
- DeZotti, G., & Gaskell, C.M. 1985, *Astron. & Astrophy.*, 147, 1
- Elvis, M., Plummer, D., Schachter, J., & Fabiano, G. 1992, *ApJS*, 80, 257
- Fasano, G., Amico, P., Bertola, F., Vio, R., & Zeilinger, W. W. 1993, *MNRAS*, 262, 109
- Harris, D. E., ed. 1984, *Einstein Observatory Revised User's Manual*, Smithsonian Astrophysical Observatory
- Ho, L. 1996, in press in *The Physics of LINERs in View of Recent Observations*, eds. Eracleous, M., Koratkar, A. P., Ho, L. C., & Leitherer, C. (San Francisco: ASP)
- Huchra, J., & Burg, R. 1992, *ApJ*, 393, 90
- Israel, F. P., van Dishoeck, E. F., Baas, F., Koornneef, J., Black, J. H., & De Graauw, T. 1990, *A&A*, 227, 342
- Jedrzejewski 1987, *MNRAS*, 226, 747
- Keel, W. 1980, *AJ*, 85, 3, 198
- Kenney, J. 1996, in *Barred Galaxies*, IAU Colloquium 157, eds. Buta, R., Crocker, D. A., & Elmegreen, B. G. (San Francisco: ASP), p. 150
- Kirhakos, S. D., & Steiner, J. E. 1990a, *AJ*, 99, 1435
- Kirhakos, S. D., & Steiner, J. E. 1990b, *AJ*, 99, 1722
- Kotilainen, J. K., Ward, M. J., Boisson, C., Depoy, D. L., Bryant, L. R., & Smith, M. G. 1992, *MNRAS*, 256, 125
- Lawrence, A., & Elvis, M. 1982, *ApJ*, 256, 410
- Maiolino, R., & Rieke, G. 1995, *ApJ*, 454, 95
- Malkan, M. A., Margon, B., & Chanan, G. A. 1984, *ApJ*, 280, 66
- Maoz, D., Filippenko, A. V., Ho, L. C., Macchetto, F. D., Rix, H.-W., & Schneider, D. P. 1996, *ApJS*, 107, 215
- McLeod, K. K., & Rieke, G. H. 1994, *ApJ*, 420, 58
- McLeod, K. K., & Rieke, G. H. 1995, *ApJ*, 441, 96
- Morse, J. A., Wilson, A. S., Elvis, M., & Weaver, K. A. 1995, *ApJ*, 439, 121
- Mukai, K. 1993, *Legacy* 3, 21-31
- Perlman, E. S. et al. 1996, *ApJS*, 104, 251
- Petre, R., Mushotzky, R. F., Krolik, J. H., & Holt, S. S. 1984, *ApJ*, 280, 499
- Piccinotti, G., Mushotzky, R. F., Boldt, E. A., Holt, S. S., Marshall, E. E., Serlemitsos, R. J., & Shafer, R. A., 1982, *ApJ*, 253, 485
- Plummer, D., Schachter, J., Garcia, M., & Elvis, M. 1994, CD-ROM issued by Smithsonian Astrophysical Observatory.
- Rix, H.-W., & Zaritsky, D. 1995, *ApJ*, 447, 82
- Rydbeck, G., Wiklind, T., Cameron, M., Wild, W., Eckart, A., Genzel, R., Rothermel, H. 1993, *A&A*, 270, L13
- Savage, B., & Mathis, J. 1979, *ARA&A*, 17, 73

- Schmitt, H. R., Kinney, A. L., Storchi-Bergmann, T., & Antonucci, R. 1996, preprint
- Scoville, N. Z., Thakkar, D., Carlstrom, J. E., & Sargent, A. I., 1993, ApJ, 404, L59
- Tacconi, L. J., Genzel, R., Blietz, M., Cameron, M., Harris, A. I., & Madden, S. 1994, ApJ, 426, 77
- Ulvestad, J. S., & Wilson, A. S. 1984, ApJ, 285, 439
- Wilson, A. S., & Tsvetanov, Z. I. 1994, AJ, 107, 1227
- Zitelli, V., Granato, G. L., Mandolesi, N., Wade, R., & Danese, L. 1993, ApJS, 84, 185

TABLE 1  
EINSTEIN SLEW SURVEY AGN WITH  $z < 0.1$

1ES Number	$b/a$ This Paper	Reason Excluded <sup>1</sup>	$b/a$ NED	$z$ NED <sup>2</sup>	Other Designations NED	Seyfert Type <sup>2</sup>
1ES0003+199	0.88	...	1.0	0.025	Mkn 335	1.0
1ES0008+107	...	sr	...	0.089	III Zw 2, Mkn 1501	1.0
1ES0048+291	0.90	...	1.0	0.036	UGC 524	1.0
1ES0050+124	0.93	...	1.0	0.061	1 Zw 1, Mkn 1502	NLSy1
1ES0057+315	0.85	...	0.5	0.015	Mkn 352	1.0
1ES0121-590	0.87	...	0.87	0.045	FAIR 9	1.0
1ES0124+189	0.92	...	0.83	0.017	Mkn 359	NLSy1
1ES0138+391	0.52	r	...	0.080	B2 0138+39B	1.0
1ES0152+022 <sup>3</sup>	...	s	...	0.08 <sup>†</sup>	...	1.0
1ES0206+522	...	s	...	0.049	GPX 02	1.0
1ES0212-010	0.87	...	0.9	0.027	NGC 863, Mkn 590	1.5
1ES0225+310	0.24	...	0.21	0.016	NGC 931, Mkn 1040	1.5
1ES0232-090	...	m (pec)	...	0.043	NGC 985	1.5
1ES0235+016	0.90	...	0.9	0.024	NGC 1019	1.0
1ES0238+069	0.72	...	...	0.028	Mkn 595	1.0
1ES0240-002	0.88	...	0.84	0.003	NGC 1068,M 77	2.0
1ES0241+622	...	sr	...	0.044	4U 0241+61	1.0 (QSO)
1ES0328+054 <sup>3</sup>	...	s	...	0.044 <sup>†</sup>	...	NLSy1
1ES0339-214	...	f	0.7	0.015	MS, ESO548-G0810	...
1ES0403-373 <sup>3</sup>	0.49 <sup>5</sup>	...	0.2	0.055	FAIR 1119	1.5
1ES0414+379	...	sr	...	0.048	3C 111.0	1.0
1ES0418-550	...	...	0.80	0.005	NGC 1566	1.5
1ES0429-537	0.90	m (Epec)	...	0.040	FAIR 303	1.0
1ES0430+052	0.66	r	0.75	0.033	Mkn 1506, 3C120	1.0
1ES0435-472 <sup>3</sup>	0.79	...	...	0.05 <sup>†</sup>	...	1.2
1ES0439-085 <sup>3</sup>	...	s	...	0.05 <sup>†</sup>	...	1.2-1.5
1ES0459+034	0.76	...	...	0.016	GHIGO, MS 0459.5+0327	1.5
1ES0513-002	0.84	...	0.72	0.033	Mkn 1095, AKN 120	1.0
1ES0518-458	0.62	r	0.75	0.034	Pic. A	1.0
1ES0545-336 <sup>3</sup>	0.43	...	...	0.03 <sup>†</sup>	...	1.8
1ES0639-756 <sup>3</sup>	0.66	...	...	0.09 <sup>†</sup>	...	1.8
1ES0655+542	0.65	m (interacting)	0.42	0.044	Mkn 374	1.5
1ES0702+646	0.78	...	...	0.079	VII Zw 118	1.0
1ES0752+393	0.90	...	0.88	0.034	Mkn 382	1.0
1ES0804+761	0.85	...	...	0.099	PG0804+761	1.0 (QSO)
1ES0818+544	...	s	...	0.086	MS, IRAS F08187+5428	...
1ES0844+349	0.75 <sup>**</sup>	...	...	0.064	PG0844+349	1.0 (QSO)
1ES0849+080	0.69 <sup>**</sup>	...	...	0.063	MS0849.5+0805	1.0
1ES0915-118	...	fr	1.0	0.055	Hydra A	RG
1ES0915+165	0.58	...	0.57	0.029	Mkn 704	1.5
1ES0921+525	...	m (interacting)	0.4	0.036	Mkn 110	1.0
1ES0923+129	0.83	...	0.85	0.028	Mkn 705	1.0

TABLE 1—*Continued*

1ES Number	$b/a$ This Paper	Reason Excluded <sup>1</sup>	$b/a$ NED	$z$ NED <sup>2</sup>	Other Designations NED	Seyfert Type <sup>2</sup>
1ES0942+098	0.69	...	...	0.013	MS 0942.8+0950	1.9
1ES0943-140	...	...	0.31	0.008	NGC 2992	2.0
1ES0951+693	...	...	0.52	0.001	M 81, NGC 3031	1.9
1ES1020+201	...	...	0.66	0.004	NGC 3227	1.5
1ES1022+519	0.80	...	...	0.045	Mkn 142	1.0
1ES1103+728	0.76	...	0.76	0.009	NGC 3516	1.2
1ES1136-374	0.89	...	0.89	0.009	NGC 3783	1.2
1ES1136+342	0.72	...	0.83	0.033	KUG 1136+342	1.5
1ES1141+799 <sup>3</sup>	0.70	...	0.63	0.065 <sup>†</sup>	UGC 6728	1.2
1ES1149-110	0.40	...	...	0.049	PG1149-110	1.0
1ES1155+557	0.79	...	0.81	0.003	NGC 3998	1.0/LINER?
1ES1200+448	0.76	...	0.75	0.002	NGC 4051	1.5
1ES1208+396	...	...	0.71	0.003	NGC 4151	1.5
1ES1211+143	1.0**	...	...	0.085	PG1211+143	1.0 (QSO/NLSy1)
1ES1215+300	0.78	...	0.8	0.012	NGC 4253, Mkn 766	NLSy1
1ES1219+755	...	f	...	0.070	Mkn 205	1.0
1ES1235+120	0.80	...	0.79	0.005	NGC 4579	1.9
1ES1238-332 <sup>3</sup>	0.22	...	0.2	0.050 <sup>†</sup>	ESO 381-7	1.5
1ES1244+026	...	s	...	0.048	PG1244+026	1.0
1ES1249-131	...	m (interacting)	...	0.014	IRAS 1249-13	1.5
1ES1257+286	...	s	...	0.092	X COM	1.0
1ES1320+084	0.86	...	...	0.050 <sup>†</sup>	Mkn 1347	1.0
1ES1322-427	...	mr (S0pec)	0.78	0.002	Cen A	2.0
1ES1323+717 <sup>3,4</sup>	0.48	...	...	0.072	Z 1323+7145	2.0?
1ES1324-268 <sup>3</sup>	...	m (Irr)	...	0.050 <sup>†</sup>	ESO 509-14	...
1ES1333-340	0.61	...	0.6	0.008	MCG-6-30-15	1.0
1ES1346-300	0.35	...	0.28	0.014	IC 4329A	1.0
1ES1351+400	...	s	...	0.062	MS 1351.6+4005	...
1ES1351+695	0.65	...	0.56	0.031	Mkn 279	1.0
1ES1410-029	0.25	...	0.32	0.006	NGC 5506, Mkn 1376	1.9
1ES1426+015	0.75**	...	...	0.086	Mkn 1383, PG 1426+015	1.0 (QSO)
1ES1501+106	0.92 *	m (E)	...	0.036	Mkn 841	1.5
1ES1518+593	0.55 *	...	...	0.079	SBS 1518+593	1.0
1ES1539+187 <sup>3</sup>	...	s	...	0.070 <sup>†</sup>	...	1.2-1.5
1ES1615+061	0.30 *	...	...	0.038	IRAS 16154+0611	1.0
1ES1618+411 <sup>3</sup>	0.54 *	...	0.75	0.036 <sup>†</sup>	KUG 1618+410	1.2
1ES1622+261	... *	m (interacting)	...	0.040	EXO, IRAS F16221+2611	2.0?
1ES1659+341 <sup>3</sup>	...	s	...	0.09 <sup>†</sup>	...	1.5
1ES1702+457	0.47	...	...	0.059 <sup>†</sup>	IRAS 17020+4544	NLSy1
1ES1720+309	0.72 *	...	0.63	0.043	Mkn 506	1.5
1ES1739+518	0.46 *	...	...	0.061	E1739+518	1.0
1ES1743+480 <sup>3</sup>	0.53	...	...	0.053 <sup>†</sup>	IRAS F17437+4803	NLSy1
1ES1817+537 <sup>3</sup>	... *	s	...	0.08 <sup>†</sup>	IRAS 18171+5342	1.0

TABLE 1—*Continued*

1ES Number	$b/a$ This Paper	Reason Excluded <sup>1</sup>	$b/a$ NED	$z$ NED <sup>2</sup>	Other Designations NED	Seyfert Type <sup>2</sup>
1ES1833+326	0.88 *	r	...	0.059	3C 282.0	1.0
1ES1845+797	0.84	r	...	0.057	3C 390.3	1.0
1ES1927+654 <sup>3</sup>	...	f	...	0.017 <sup>†</sup>	...	1.9-2
1ES1934-063	0.84	...	...	0.011	SS 442	2.0?
1ES1957+405	... *	fr	...	0.058	Cyg A	2.0
1ES2055+298 <sup>3</sup>	0.51	...	...	0.036 <sup>†</sup>	...	NLSy1
1ES2137+241 <sup>3</sup>	0.52	...	...	0.037 <sup>†</sup>	...	NLSy1?
1ES2240+294	0.79	...	0.57	0.025	ARK 564	NLSy1
1ES2251-178	...	s	...	0.068	MR 2251-178	1.0(QSO)
1ES2254-371	0.84	...	...	0.039	MS 2254.9-3712	...
1ES2304+042	0.70	...	...	0.042	PG2304+042	1.0

<sup>1</sup>Object excluded from one or more subsamples for the following reason: (f) foreground contamination; (m) morphological type not spiral (type information in parentheses); (r) radio source; (s) too small for reliable determination of  $b/a$ . See text.

<sup>2</sup>From NED and other literature unless marked with a †, in which case derived from Slew Survey spectra. Note that the spectra from which the Seyfert types were identified are not always of sufficient quality to distinguish among subtypes.

<sup>3</sup>Not known as a Seyfert before the Slew Survey.

<sup>4</sup>1ES1323+717 was located outside the 2' 95% error circle of the Slew Survey.

<sup>5</sup>Our axial ratio measurement for 1ES0403-373 is likely an upper limit; we adopt the NED value for statistical use.

\*CCD image obtained for this object.

\*\*IR image used to measure axial ratio.

TABLE 2  
KS PROBABILITIES AMONG AGN SAMPLES

	Hard X-ray 26 objects	Soft X-ray 44 objects	UV 56 objects	Visible 42 objects
Random orientations	0.045	$3 \times 10^{-6}$	$7 \times 10^{-11}$	$2 \times 10^{-12}$
Hard X-ray	...	0.358	0.043	0.011
Soft X-ray	...	...	0.669	0.054
UV	...	...	...	0.349